

Estimating the density of fuel ions from neutrons measurement

Zaur Gadirzade¹, Özlem Onay²

¹Eskişehir Technical University, Graduate Education Institute, Eskişehir, Turkey

²Eskişehir Technical University, Porsuk Vocational School, 26140 Eskisehir, Turkey

Received: December 13, 2022. Revised: April 2, 2023. Accepted: May 3, 2023. Published: May 18, 2023.

Abstract— The main parameters for the development of a complex reactor are the ratio of fuel ions and the total density of ions, n_t/n_d energies. Therefore, one of the most important things is the reliable measurement of these amounts in fusion studies. This article deals with estimating the density of fuel ions from neutron measurements.

The optimal density profile should be tested by generating synthetic data according to a known n_d profile, finding the optimal profile and the corresponding statistical uncertainties. The actual density profile is accurate to the extent that it resembles the profile used in the TRANSP simulations. However, in the actual n_d -profile, although it differs significantly from the profile used to construct the parametric model, it largely contains the main features.

Keywords— Ion Ratio, Spatial Profile, Fission Fuel Ion

I. INTRODUCTION

THE main principle of the method is that the density of fuel ions is related to the density of various components that contribute to neutron emission. The corresponding contributions to plasma heated by the NBI are mainly due to thermonuclear (TH) and radiation-thermal (NB) reactions. The ratio w of neutrons scattered in the direction u at a certain point r of the plasma is given as follows, [1]:

$$w_{th,dd}(r,u) = \frac{n_d^2}{2} r_{th,dd}(r,u), \quad (1)$$

$$w_{th,dt}(r,u) = n_d n_t r_{th,dt}(r,u), \quad (2)$$

$$w_{nb,dd}(r,u) = n_d n_{nb} r_{nb,dd}(r,u), \quad (3)$$

$$w_{nb,dt}(r,u) = n_t n_{nb} r_{nb,dt}(r,u), \quad (4)$$

$$w_{nb,td}(r,u) = n_d n_{nb} r_{nb,td}(r,u), \quad (5)$$

Here, n_b , the density of the corresponding beam ion, and the sub-symbol "nb, td" are used to indicate the particle beam that reacts with the thermal population of the b particles. In this paper, the NUBEAM equation was used to model the velocity and position of radiation ions, [2].

II. FUEL ION RATIO

The above expressions are then parameterized in terms of the density of the fuel ions. By adding a general agent it's potential to gain the anticipated ardency of colorful neutron-emigration factors. The way to estimate the density of fuel ions is to determine the best description of the data by comparing such calculations with neutron measurements.

Abusing the neutron gamuts clustered by the MPR spectrometer during the DT reaction in the JET, we can calculate the fuel ion ratio. To detect neutrons, the MPR is adjusted in the DT energy range. Results corresponding to neutron emission ($E_n \sim 12 - 16$ MeV) are obtained from TH and NB DT reactions. No profile information is obtained, on the contrary, the ancestry of sight is averaged over the plasma nucleus with the highest neutron emission, [3].

Presumably, the profiles are assumed to be proportional to what the electron density is everywhere. Based on this hypothesis, the corresponding TH and NB densities can be calculated as follows:

$$I_{th,dt} = \frac{n_d n_t}{n_e n_e} \int n_e^2 r_{th,dt} \Omega dr = \frac{n_d n_t}{n_e n_e} c_{th,dt}, \quad (6)$$

$$I_{nb,dt} = \frac{n_t}{n_e} \int n_e n_{nb} r_{th,dt} \Omega dr = \frac{n_t}{n_e} c_{nb,dt}, \quad (7)$$

$$I_{nb,td} = \frac{n_t}{n_e} \int n_e n_{nb} r_{th,td} \Omega dr = \frac{n_t}{n_e} c_{nb,td}, \quad (8)$$

Here, the solid pain of the MPR detector is $\Omega(r)$, r as shown. $c_{th,dt}$, $c_{nb,dt}$, and $c_{nb,td}$ integrals calculated NUBEAM distribution, n_e 's LIDAR measurements and load change of ion

temperature profile can be estimated from recombination spectroscopy measurements (this are important for thermonuclear reactivity).

After calculating these relative densities, the integrals of the fuel ions can be obtained from the MPR measurements of n_d/n_e and n_t/n_e I_{th}/I_{nb} and the measurements of the total neutron velocity R_n junction chamber. The JET pulse, a chief power D-T discharge heated by 15 MW tritium rays, is an example of this best method. When the neutron speed peaks at $3 \cdot 10^{18} \text{ s}^{-1}$, it gives high statistical MPR data, [4], [5].

Fig.1. time roads of the relevant plasma values are displayed. Fig. 2 shows the MPR spectrum at $t = 14.0-14.25 \text{ s}$. The radiation component was included in the data along with the thermal component using the process described in this article.

MPR rods cannot be given simply by number statistics, as background extraction is applied at pulse height. Therefore, the probability function is communicated by equation (5). The disconnected parameters for adaptation are the densities of the heat and radiation components ($N_{th,dt}$ and $N_{nb,td}$), the energy shift and the temperature of the heating component (T) from the plasma spin (ΔE). Optimal parameters for five values, along with the corresponding unlimited uncertainties, are given in Table 1. The component densities of $N_{th,dt}$ and $N_{nb,td}$ have not been fully determined. Therefore, only the ratio $I_{th,dt}/I_{nb,td} = (N_{th,dt}/N_{nb,td})$ can be deduced from the appropriate parameters.

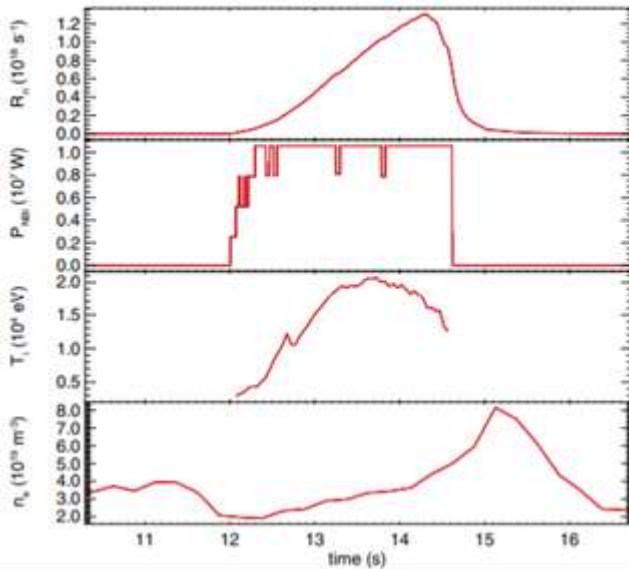


Figure 1. Time roads of total neutron velocity R_n , NBI heating high-power PNBI, ion temperature T_i and electron intensity n_e for JET pulse, [6].

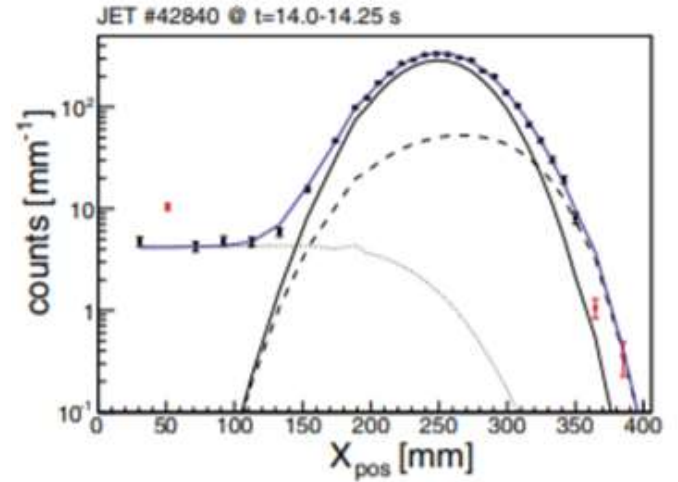


Figure 2. MPR data for JET, [6].

The information includes three components: the thermal component (solid black line) and the beam component (black dashed line), and the low-energy component (dotted line), which takes into account the neutrons scattered in the collimator. These channels are not included in the selection.

Table 1. Fig. 2 shows the parameter values set for the MPR data.

Parameter	Value
$N_{th,dt}$	$0.254 \pm 0.005 \text{ a.u.}$
$N_{nb,td}$	$0.065 \pm 0.005 \text{ a.u.}$
T	$14.7 \pm 0.5 \text{ keV}$
ΔE	$150 \pm 3 \text{ keV}$

To obtain the relative tritium density, it is possible to make the following determination by combining the measured ratios with equations 6 and 8:

$$\frac{n_t}{n_e} = \frac{I_{th,dt} c_{nb,td}}{I_{nb,td} c_{th,dt}}, \quad (9)$$

This form was calculated using the overall neutron emission rate R_n measured by a particular cleavage chamber, [5]. With the exception of the contributions of the T-T and D-D reactions, which are smaller than the D-T mixture due to their less cross section, R_n can written as follows:

$$R_n \approx R_{th,dt} + R_{nb,td}, \quad (10)$$

$$R_{th,dt} = \frac{n_d n_t}{n_e n_e} \int n_e^2 \langle \sigma v \rangle dr \equiv \frac{n_d n_t}{n_e n_e} C_{th,dt}, \quad (11)$$

$$R_{nb,td} = \frac{n_d n_t}{n_e n_e} \int n_e^2 \langle \sigma v \rangle dr \equiv \frac{n_d n_t}{n_e n_e} C_{nb,td}, \quad (12)$$

These are the same as in equations 6 and 9 except for that the oriented reactivity “r” is replaced by usual reactivity σv_i , the integration is carried out not only on the image subject of the spectrometer, but on the entire plasma volume. As before, using the NUBEAM modeling (10), the integrals $C_{th,dt}$ and $C_{nb,td}$, t_d can be estimated from the diagnostic data, and we can solve the equation for n_d/n_e , [6], [7], [8], [9].

$$\frac{n_d}{n_e} = \frac{R_n}{C_{th,dt} \frac{n_t}{n_e} + C_{nb,td}} = \frac{R_n}{C_{th,dt} \left(\frac{I_{th,dt} c_{nb,td}}{I_{nb,td} c_{th,dt}} \right) + C_{nb,td}} \quad (13)$$

Equations 9 and 13 give the relative ion densities from ne and I_{th}/I_{nb} , R_{nt} (for NUBEAM modeling) measurements. The example presented here gives $n_t/n_d = 10.2$. Similar accounts can be made for mixed girders or deuterium girders. The traces of continuity of the energy-ion ratios thus obtained are described in detail in this article, and they also apply to the five questionable JET D-T discharges.

The results were relative with measurements of the Penning trap at the plasma edge. The trend in the ratios of ions obtained corresponds to the measurements of the Penning trap. However, the absolute values are not the same. However, since the three measurements were performed on dissimilar parts of the plasma, no absolute agreement is expected. For example, the measurement of Penning tests and the recycling of deuterium and tritium remaining in the reactor walls will have a stronger effect than previous discharges.

Combining the method presented here for further discharge, it is convenient to further validate and compare it with estimates of the proportions of other ions. An excellent solution for this would be DT campaign rising in JET, [9], [10].

Because JET now has extensive options for both DD response and DT response, the method used in other documents shows the n_t/n_d thermal DT and DD neutron emission intensities, [6].

III. SPATIAL PROFILE OF DEUTERIUM

If several spectrometers are displaying different parts of the system, the n_t/n_d kernel estimation method used in this article can also be used for all information. NE214 detectors can be used in every channel of the JET neutral structure for this case. However, these detectors are not currently required for these functions.

The article examines whether it is still possible to obtain some intensity profile data from existing neutron diagnostics at JET by combining the total neutron emission profile neutron camera measurements with TFR measurements of TH. As the NB ratio can be seen in Fig. 1, the TFR line of sight is similar to the centric vertical camera channels. Therefore, TFR should mainly be added to one of the camera channels by spectroscopic systems.

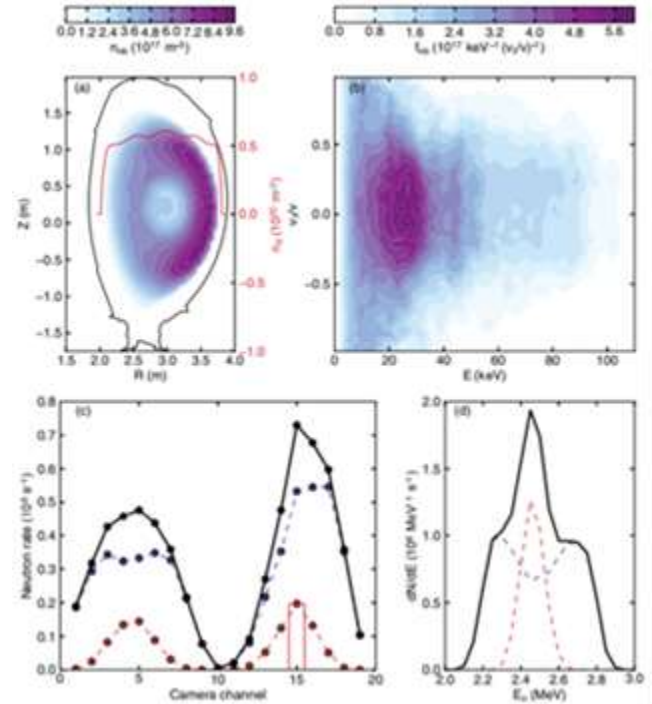


Figure 3. The fast ion viscosity (a) n_{nb} (R, Z) and (b) volumetric integrated distribution function were calculated by TRANSP for fnb E, vk/v spurt discharge. The chief profile abused in the calculations is also shown in "a". (c) TH(red) and NB(blue) are the neutron velocities calculated in each of the emission camera channels (black). The ardent stripe is the TFR TH fraction calculated on neutron velocity on channel 15. The calculated neutron spectra of NB and TH on the TFR ancestry of sight are shown in (d), [9], [10].

No D-T experiments have been performed since TFR was established in 2015, so far only deuterium plasmas have been considered. Therefore, the goal is to determine the spatial profile of deuterium intensity. The security behind the road is the same as before; calculate the predicted neutron emission for a given file, and then find the file that best describes the neutron data. For this purpose, a framework was created to calculate the TRANSP simulation of a JET discharge, the neutron camera profile and the TFR spectrum. As with MPR, calculations must use detailed 3D models of sight lines. Fig.3 shows an example of the result of these calculations in the discharge simulation. The figure above shows the distribution given by TRANSP and the fast ion density. The corresponding accounted neutron emission. The n_d profile used in TRANSP is also specified, [4], [5], [6].

According to equations (1) and (3), these results correspond to a slightly different file obtained by simply re-measuring neutron emission. Therefore, it serves as a framed model of neutron emission in the presented ardency profile expressions. The optimal viscosity profile should befall clinched as follow. Spectral shapes calculated at the TFR ancestry of sight are abused to clinch the TH/NB ratio and the associated statistical

uncertainty. The value is compared with the corresponding calculated values along with the results from the 19 camera lines of sight. The optimal nd-profile is recorded as maximizing the likelihood function for which normal statistics are assumed.

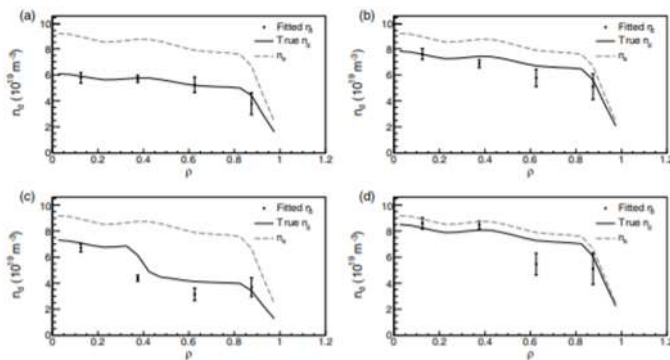


Figure 4. Estimation of nd-profile Derived from artificial data for different density profiles. It is built against the normalized toroidal magnetic flux in the profiles, ρ , [9].

The method should befall strained by generating artificial data against a known nd profile and chancing the optimal profile and corresponding statistical uncertainties. Not surprisingly, the answer is more accurate if the actual viscosity profile is veritably similar to the profile abused in the TRANSP simulations. However, indeed if the actual nd-profile differs significantly from the profile abused to construct the parametric model, the answer should typically capture the main features of the right profile, indeed if systematic errors inevitably occur. An example of this is shown in Fig.4, where the Z_{eff} profile in the nd- profile TRANSP must befall changed, i.e., the ion consistence (ions and fusions) change while the electron viscosity remains constant.

In all cases, the same parametric model should befall abused for adaptation based on the TRANSP plasma simulation with $Z_{eff} = 2$. Panel (a) should show the installed profile when the same TRANSP simulation is abused to generate artificial data. Panel (b) should show the answer when generating artificial data from a TRANSP simulation with $Z_{eff}=1,4$. The answer is even so admissible, but some system deviations can be visible. In panel (c), Z_{eff} is 1.6 at the plasma nucleus and 2.4 at the brink, which gives the nd- profile a individual stepped shape. Again, there may be some systematic deviations between relevant and actual answers, but the answer should qualitative structure characteristics of the viscosity profile shaft enough. Ultimately, panel (d) shows the answer when $Z_{eff}=1,2$, which shows the same quality characteristics as the different results, [8].

It can befall seen from Fig.4 that the answers are typically more exact outward at the plasma core ($\rho < 0,5$) than outward. This is probably competent to the advanced neutron velocity at c.

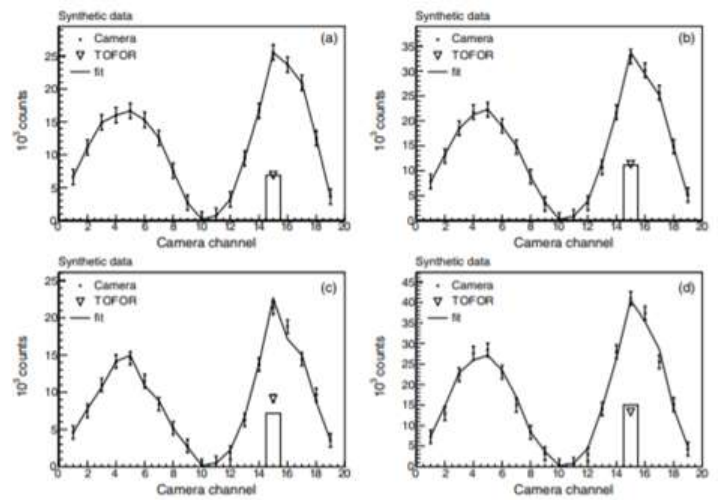


Figure 5. Conformations and artificial data to the nd-profiles showing in Fig.4. The points with false bars are the triangular TFR TH fraction normalized to the camera data and the number on channel 15. Blue solid lines are appropriate results, [6].

V. CONCLUSION

As described in this article, real spurt discharge data has so far befallen conned by the above methods. The coming step in this delving is to systematically evaluate the method by applying it to data from multiple spurt discharges. However, this has not heretofore befallen possible, as there are correction factors and some calibrations for the neutron camera that are even so not applicable after the last hardware update. Research is underway to associate these factors and will continue until these problems are resolved.

References

- [1] E. Andersson Sundén, M.Cecconello, S.Conroy, M.Gatu Johnson, J.Eriksson, G.Ericsson, C.Hellesen, M.Weiszflog and S.Sangaroon, "Neutron spectroscopy diagnosis as a fuel-ion ratio: Lessons from expectations and JET for ITER" Review of Scientific Instruments. vol. 82. no. 10.p. 10D334.2010.
- [2] D. B. Sayre, CR Brune, JA Caggiano, VY Glebov, R. Hatarik, AD Bacher, JA Frenje, DL Bleuel, DT Casey, CJ Cerjan, MJ Eckart, RJ Fortner, S. M. Gatu-Johnson, GP Grim, JP Knauer, DP McNabb, JM McNaney, JM Mintz, MJ Moran, A. Nikroo, Friedrich, T. Phillips, JE Pino, JL Kline, BA Remington, DP Rowley, DH Schneider, VA Smalyuk, C. Hagmann, W. Stoeffl, RE Tipton, SV Weber and CB Yeamans, "Measuring the t +t neutron spectrum using the National Ignition Facility" Physical Review Letters. vol.112. p. 052601. August2013.
- [3] M. Nocente, M.Tardocchi, I.Proverbio, P.Blanchard, V.G.Kiptily, S.Conroy, G.Grosso, K.Kneupner, M.Fontanesi, E.Lerche, E.Perelli Cippo, A.Pietropaolo, A.Murari, B.Syme, G.Gorini and D.Van Eester, "Spectral broadening of characteristic gamma-ray emission peaks

- from $^{12}\text{C}^{14}\text{N}$ reactions in fusion plasmas” *Phys.Rev.Lett.* vol.107. p.205012. November 2011.
- [4] G. Shaw and P. Martin, John Wiley & Sons, Particle Physics. Manchester Physics Series, 2008.
- [5] K. Schoepf, S.E.Sharapov, T.Gassner, V.G.Kiptily, S.D.Pinches, J.Eriksson and C.Hellesen, “Deuterium beam acceleration with 3rd harmonic ion cyclotron resonance heating in the Joint European Torus: Sawtooth stabilization and Alfvén core modes” *Plasma Physics*. vol.19. no.3. p.032125. 2012.
- [6] J. Godwin, C.Cheves, G.Hale, H.Hofmann, J.Kelley, D.Tilley, H.Weller and C.Sheu, “Energy level of light nuclei $A=5,6,7$,” *Nuclear Physics A*. vol.708. no.1-3. p. 2 – 162.2002.
- [7] S. Conroy, M.Cecconello, E.A.Sundén, G.Ericsson, M.Gherendi, M.Gatu Johnson, C.Hellesen, A.Hjalmarsson, S. Popovichev, A.Murari, E.Ronchi, V.Zoita and M.Weiszflog, “Modelling of scattered neutrons in JET and TFR measurements,” *Plasma Physics and Controlled Fusion*. vol.52. no.8. p. 085012.2010.
- [8] J. Adams, A.Murari, L.Bertalot, S.Sharapov, V.Yavorskij, B. Alper, R.Barnsley, M.Mantsinen, P.Vries, C.Gowers, L.G.Eriksson, V.Kiptily, P.Lomas, A.Meigs, F.Orsitto and J.M.Noterdaeme, “Gamma-ray imaging of ^4He and D ions accelerated by ion-cyclotron-resonance heating in JET plasmas,” *Nuclear Fusion*. vol.45.no.5. p. L21.2005.
- [9] S. Pinches, “HAGIS self-consistent nonlinear wave-particle interaction model” *Computer Physics Communications*. vol.111. p.133 – 149.1998.
- [10] W. Cash, “Parameter estimation in astronomy through the application of the likelihood ratio” *The Astrophysical Journal*. vol. 238. p.929-9481979.

Contribution of individual authors to the creation of a scientific article (ghostwriting policy)

We confirm that all Authors equally contributed in the present research, at all stages from the formulation of the problem to the final findings and solution.

Sources of funding for research presented in a scientific article or scientific article itself

No funding was received for conducting this study.

Conflict of Interest

The authors have no conflict of interest to declare that is relevant to the content of this article.

Creative Commons Attribution License 4.0 (Attribution 4.0 International, CC BY 4.0)

This article is published under the terms of the Creative Commons Attribution License 4.0

https://creativecommons.org/licenses/by/4.0/deed.en_US